

Detecting new Buffel grass infestations in Australian arid lands: evaluation of methods using high-resolution multispectral imagery and aerial photography

V. M. Marshall · M. M. Lewis · B. Ostendorf

Received: 15 February 2013 / Accepted: 30 September 2013 / Published online: 14 November 2013
© The Author(s) 2013. This article is published with open access at Springerlink.com

Abstract We assess the feasibility of using airborne imagery for Buffel grass detection in Australian arid lands and evaluate four commonly used image classification techniques (visual estimate, manual digitisation, unsupervised classification and normalised difference vegetation index (NDVI) thresholding) for their suitability to this purpose. Colour digital aerial photography captured at approximately 5 cm of ground sample distance (GSD) and four-band (visible–near-infrared) multispectral imagery (25 cm GSD) were acquired (14 February 2012) across overlapping subsets of our study site. In the field, Buffel grass projected cover estimates were collected for quadrates (10 m diameter), which were subsequently used to evaluate the four image classification techniques. Buffel grass was found to be widespread throughout our study site; it was particularly prevalent in riparian land systems and alluvial plains. On hill slopes, Buffel grass was often present in depressions, valleys and crevices of rock outcrops, but the spread appeared to be dependent on soil type and vegetation communities. Visual cover estimates performed best (r^2 0.39), and pixel-based classifiers (unsupervised classification and NDVI thresholding) performed worst (r^2 0.21). Manual digitising consistently underrepresented Buffel grass cover compared with field- and image-based visual cover estimates; we did not find the labours of digitising

rewarding. Our recommendation for regional documentation of new infestation of Buffel grass is to acquire ultra-high-resolution aerial photography and have a trained observer score cover against visual standards and use the scored sites to interpolate density across the region.

Keywords Remote sensing · Aerial photography · High resolution · Invasive species · Natural resource management · *Cenchrus ciliaris* · *Pennisetum ciliare*

Introduction

Encroachment of invasive Buffel grass (*Cenchrus ciliaris* L. *Pennisetum ciliare*) into arid and semi-arid ecosystems requires early detection if we are to have any hope of controlling its spread. Originally from Africa, this drought hardy bunch grass was introduced into Australia and the Americas as rangeland pasture where it remains an important resource (Brenner 2011; Smyth et al. 2009). Outside intended areas, it is a concern for natural resource managers because it accumulates dead matter, promoting fire in fire-intolerant systems, homogenising landscapes and threatening environmental and cultural values of infested areas (D'Antonio and Vitousek 1992; Miller et al. 2010).

Comprehensive species distribution maps are invaluable to the containment of all invasive species (Stohlgren and Schnase 2006). Field-based mapping is only feasible over localised areas and is typically restricted by road access, to sites of particular

V. M. Marshall (✉) · M. M. Lewis · B. Ostendorf
School of Earth and Environmental Science, The University
of Adelaide, Glen Osmond, South Australia, Australia
e-mail: victoria.marshall@adelaide.edu.au

significance, or to sites identified for strategic control (where an isolated occurrence is observed). These areas are mapped as a prelude to control within this area, and there is usually some prior knowledge on the distribution before localised mapping efforts are undertaken. In the remote desert landscapes of Australia, where Buffel grass thrives and is widespread, field-based mapping is inadequate; the alternative is a remote sensing approach.

Remote sensing has been proven as an effective tool for community-level vegetation mapping and monitoring (Brink and Eva 2009; Ramakrishna and Steven 1996; Mehner 2004). Discrimination of individual plant species is more difficult due to the complexity of species intermixing with surrounding vegetation and spectral variability within individual species. Remote sensing approaches to species-level plant mapping have been most successful when the target species possess distinctive spectra, has a large structure or grows in large stands relative to the spatial resolution of the imagery and shows vigorous population growth, and when the phenological stages of growth are taken into account during spectral signature collection (Jia et al. 2011; Wang et al. 2008; Andrew and Ustin 2008; Blumenthal et al. 2009; Hestir et al. 2008; Ustin et al. 2002; Padalia et al. 2013; Ge et al. 2006). This presents several challenges for the remote detection of Buffel grass because most grasses are spectrally similar; the size of stands is variable and with unknown limits; vigorous growth is a response to rainfall and is not strictly seasonal; and there is a degree of intra-species variation.

Nonetheless, in the Sonoran Desert of Mexico and the USA, several studies demonstrate success in remote detection of Buffel grass (Brenner et al. 2012; Franklin et al. 2006; Olsson et al. 2011). These studies primarily utilised moderate resolution satellite imagery, useful for monitoring large established infestations or pastures. Olsson et al. (2011) was able to distinguish Buffel grass in heterogeneous mixed desert scrub with the greatest success by integrating hyperspectral measurements of plant spectra collected in the field. However, these approaches are not necessarily useful for detecting new infestations as an alternative to field work.

For remote detection of emerging infestations, individual tussocks, less than 0.5 m in diameter, must be definable. This requires a high spatial resolution with a ground sample distance (GSD) that is below 25 cm, i.e. half the smallest unit to be classified (Myint et al.

2011). An advantage to using aerial imagery is that acquisition timing is extremely flexible. This is critical, when working with grasses that rapidly green up in response to rainfall, and almost as quickly dry off or burn to ash, leaving a very small window of time when imagery can be captured.

There are many challenges associated with using aerial imagery such as the limited spatial coverage (footprint) of image scenes, the quality of images being strongly weather-dependant, and the spatial coverage needing to be tailored to a specific project (Gergel et al. 2010). Further challenges include data management, processing time and cost. These factors, combined with uncertainty regarding the accuracy of classifications, means aerial imagery is underutilised by natural resource managers.

Approaches to aerial image classification vary in regard to accuracy, consistency, time consumption and required producer expertise. Visual interpretation can be highly accurate; it requires minimal image preparation and uses human knowledge to make logical decisions (Gergel et al. 2010). This method can be documented either by digitising infestations (Olsson et al. 2012) or by using visual standards to categorically record species cover at selected locations across the study site (Puckey et al. 2007). Digitising is extremely laborious but less subjective than visual cover standards (Gergel et al. 2010).

Pixel-based classifications are semi-automated, systematic, repeatable and require less interpretation time. However, these rely solely on spectral separation of the target species from surrounding land cover, which is complex in the case of this variable grass. In some ways, it is also less suited to analyses at high spatial resolutions because of the spectral diversity within the tussocks. For example, the sunlit side of tussocks may present a different spectral category to the shadowed side, or dry foliage, a different category from green foliage, resulting in a speckled “salt-and-pepper” effect (Myint et al. 2011). More recently, object-based classifiers have been developed, which, like pixel-based classifiers, are systematic, consistent and repeatable, but they better mimic human perception of objects (Walter 2004; Laliberte et al. 2004; Yu et al. 2006; Meneguzzo et al. 2012). Object-based classification algorithms are not yet well developed and require expert production.

Our goal is to explore the potential of aerial imagery for detection of Buffel grass populations in the Australian desert country. Specifically, we examine 5–6 cm (GSD)

ultra-high-resolution colour digital aerial photography and 25 cm (GSD), four-band (visible–near-infrared (NIR)) multispectral imagery. We compare four different yet common classification approaches—visual cues, manual digitisation, unsupervised classification and Normalised Difference Vegetation Index (NDVI) thresholds—and assess each for their suitability to Buffel grass discrimination. The research was conducted with the long-term aim of developing a method for early detection of Buffel grass in remote arid landscapes that could be used by natural resource managers.

Methods and materials

Focal species: Buffel grass (*C. ciliaris* L. *P. ciliare*)

Buffel grass is a perennial, summer-growing (C4) African bunch grass (Sharif-Zadeh and Murdoch 2001). It reproduces via seed and rhizomes and, as a result, can be seen in the landscape as both lone tussocks and dense monocultures. It does not drop its leaves; they accumulate at the base of the plant, often forming a ring of dry foliage around the tussock. The grass is spread by wind, water and traffic. In arid environments of Australia, where this study is based, it is typically found at highest density in riparian environments, depressions, and wherever soils are disturbed, including roadsides, construction sites and fire beds (Marshall et al. 2012). The plant responds rapidly to rain and often emerges before native grasses. It is also quick to dry-off and burn. The window for image capture of growing plants is brief; in Australia, we consider it is usually restricted to about a month after the first summer rains.

Study area

Located in the remote far north-west corner of South Australia, the study site occupies 15×12 km of the aboriginal owned Anangu Pitjantjatjara Yankunytjatjara (APY) lands. The site encompasses two indigenous communities—Kalka (26° 7'11.50"S, 129° 8'59.04"E) and Pipalyatjara (26° 9'37.45"S, 129°10'20.64"E) (Fig. 1)—with a combined population of less than 350. Climate is arid, with hot summers, mild winters and annual rainfall below 300 mm. Elevation ranges from 650 to 900 m. Plains comprise alluvial and fluvial sediments, vegetated by *Aristida* grasslands, sparsely distributed low shrubs and *Hakea* trees. These

grasslands are increasingly dominated by Buffel grass. The Tomkinson ranges (Fig. 1) comprise mafic rock dominated by *Spinifex* hummock grasses; ranges in the north-west of the study site (Fig. 1) comprise felsic rock dominated by *Enneapogon* sp. grasses.

Buffel grass was introduced by direct seeding around Kalka in October 1987, along with *Cenchrus setigerus* and native drought-tolerant shrubs, *Atriplex nummularia*, *Acacia kempeana* and *Acacia ligulata* to combat dust storms on the alluvial flats; dust became a problem after an uncontrolled wildfire burnt a substantial area near the settlements, drought followed, and vegetation never regenerated. As a result of the direct seeding in 1987, this region is now largely dominated by Buffel grass.

Imagery

Colour digital photography and four-band (visible to NIR) multispectral images were obtained over the study area. Image specifications are given in Table 1. The imagery was acquired on 14 February 2012 between 1134 and 1430 hours. Multispectral imagery was flown after the aerial photography from 1352 hours in the afternoon; consequently, shadow effects vary between the images. Conditions at the time of image capture were slightly hazy with less than 1 % high cirrus cloud cover. Buffel grass was approximately 50 % dried off on the day of image capture.

The aerial photography was acquired for a grid of 3×3 transects across the study site (north–south transects approx. 17 km; east–west transects approx. 12 km; spaced 5 km apart) (Fig. 1). Transects were positioned to capture the diversity of vegetation and geological settings while avoiding high elevations that are potentially dangerous for aerial navigation (Fig. 1). Photography was received as 930 un-georeferenced frames, in TIFF format. To save time georeferencing these frames individually, three-five frames were stitched together in the automated image matching program, Microsoft image composite editor (ICE). Image frames were exported from ICE as JPEG files, georeferenced in ArcGIS and saved as raster data using the minimum cell size for the image. These raster files were used for all subsequent analyses.

The four-band imagery, collected using the Spec Terra multispectral sensor, was acquired for three smaller areas, in highly diverse local environments, and overlapping the aerial photography flight paths

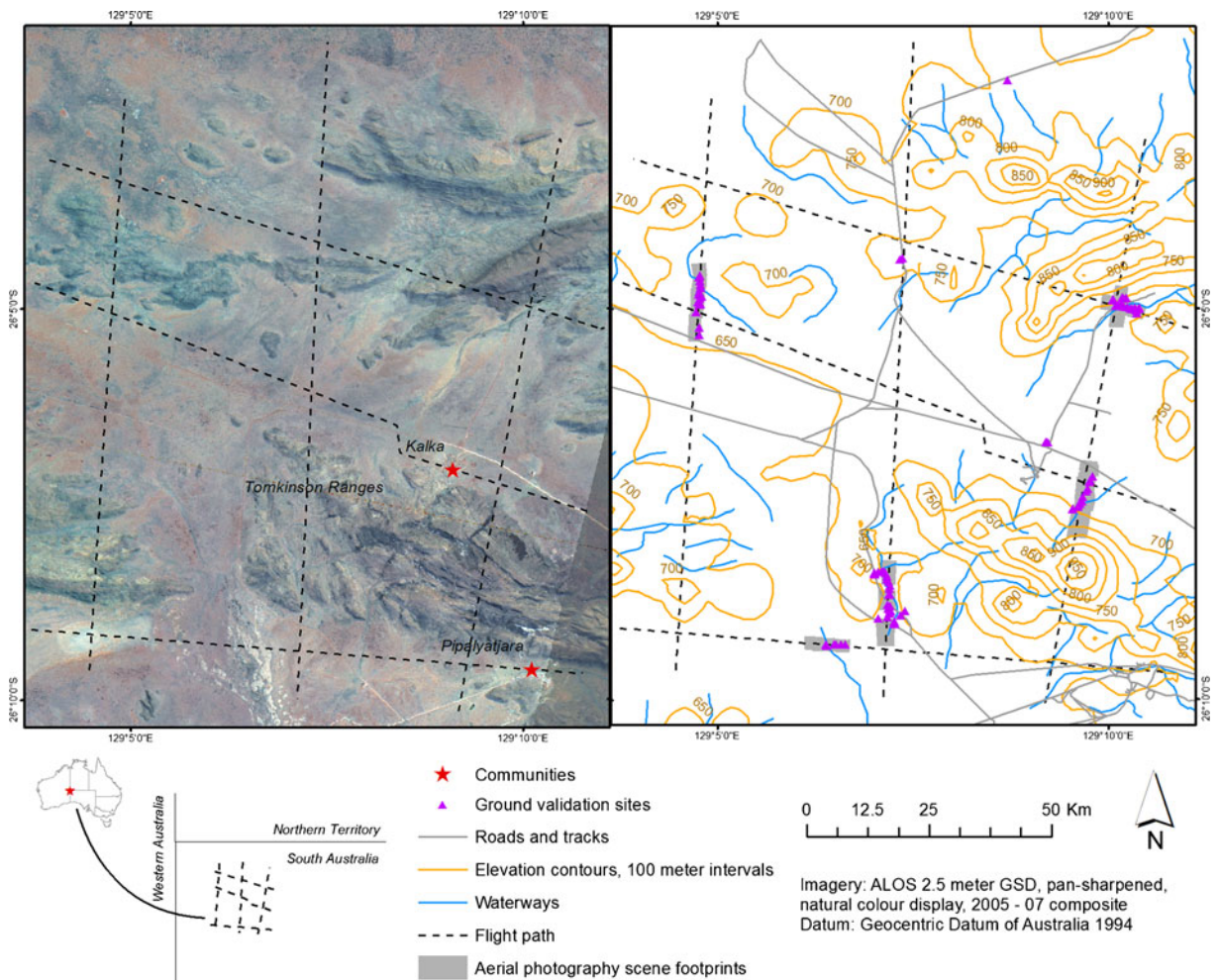


Fig. 1 Study site and flight path design. *Left:* flight paths. *Right:* field sample sites, terrain contours in which the light aircraft was navigating, and the image scenes of high quality which overlapped

(Fig. 2). The multispectral data was delivered corrected for radiometric and geometric artefacts, as orthorectified and georegistered mosaics in TIFF format. All image analysis was carried out in the 1994 Geocentric Datum of Australia, projected to UTM zone 52.

Ground validation sites

Field work was conducted from 7 to 12 February 2012. Selection of sites for ground validation was governed by in situ interpretation of environmental units, such as vegetation structure, soil colour and land use, aided by a 2007 ALOS colour mosaic of the region (2.5 m GSD). The goal was to represent the diversity of landscapes in which Buffel grass was present or absent and at varying

our field sites. These maps were prepared in the Geocentric Datum of Australia 1994

densities. In total, 95 field sites were documented. Within these circular sites (10 m in diameter), projected cover (the vertical projection of plant foliage onto a horizontal surface) was estimated for Buffel grass and land cover units categorised as “herbs and forbs”, “other grasses”, “woody”, “leaf litter” and “soil”. The cover for each cover type was recorded as discrete classes: absent, 0 %; low, 0–25 %; moderate–low, 25–55 %; moderate–high, 55–85 %; and high, 85–100 % (Fig. 3). The centre point of each ground validation site was recorded using a Garmin eTrex High Sensitivity hand-held global positioning system receiver, which achieved a spatial accuracy of approximately 2–5 m.

For remote sensing analysis, the ground validation sites were co-registered to the aerial photography and

Table 1 Image specifications for aerial imagery captured on February 2012 over the Kalka–Pip Homelands, Australia

Imagery	Sensor	Flying altitude	Footprint	Ground sample distance (GSD) or pixel size	Spectral resolution
Digital aerial photo	Nikon D3X digital camera	305 m	~240×360 m/frame	5–6 cm	Visible; 3 bands
Airborne multispectral	Spec Terra digital multispectral sensor	1,067 m	Variable	25 cm	Visible–NIR, 4 bands: 450±10 nm FWHM (blue); 550±10 nm FWHM (green); 675±10 nm FWHM (red); 780±10 nm FWHM (near-infrared)

separately to the multispectral imagery using the GPS coordinates recorded in the field and personal knowledge on the site. Of the 95 sites, 18 lay outside of the imagery

coverage. A further 41 were not used because of image quality (which diminished over hilly terrain), obstruction from trees or insufficient geographical information to

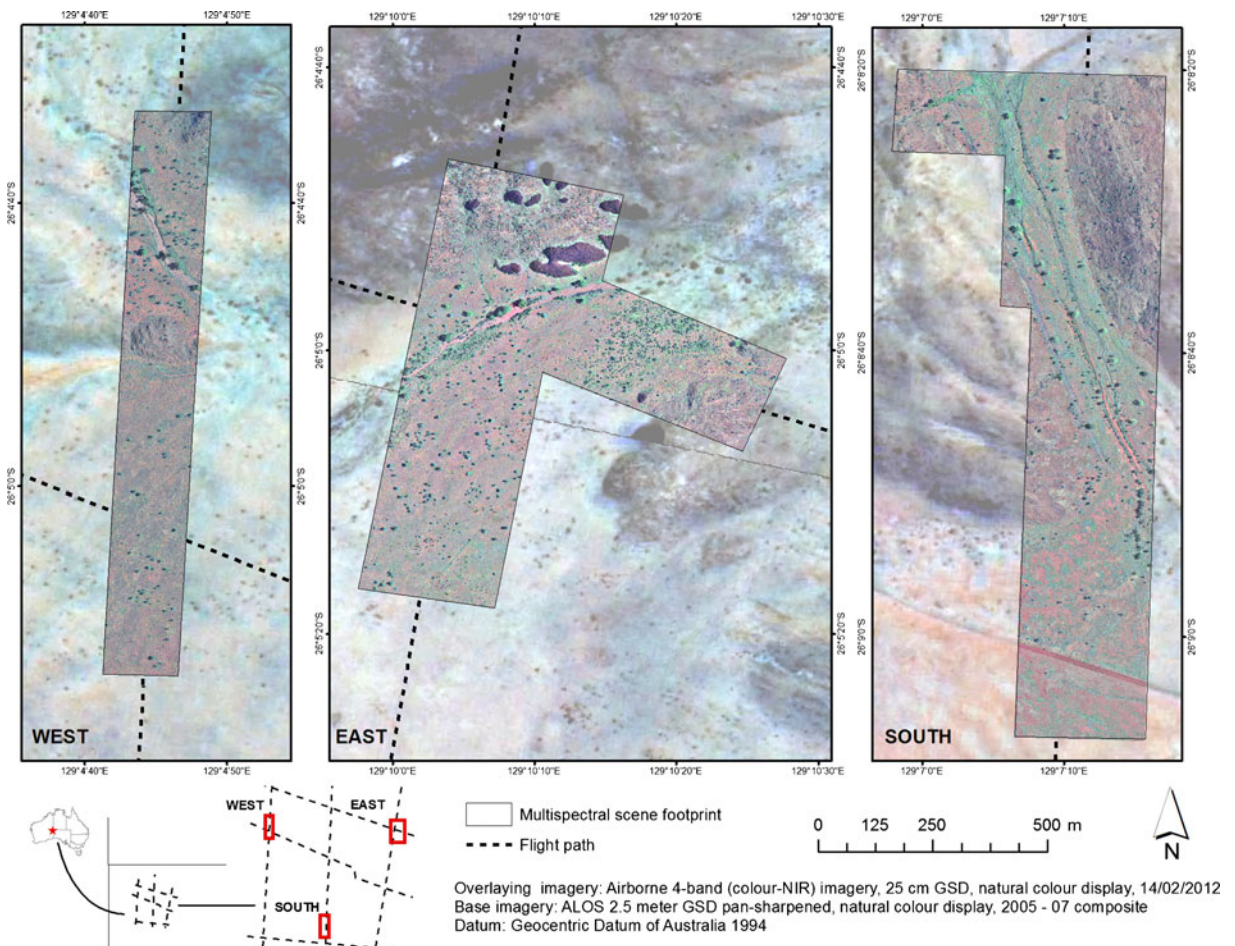


Fig. 2 Coverage of four-band Spec Terra imagery for aerial survey of Buffel grass in the Kalka–Pipalyatjara homelands of central Australia. Three Spec Terra panels were acquired in the west, east and south of the study area. These panels were designed to overlap the flight path for aerial photography collection and

represent the varied landscape. The Spec Terra data is presented with a natural-colour display. The underlying image on all three maps is ALOS 2.5 m GSD pan-sharpened imagery, 2005–2007 composite, natural-colour display. These maps are prepared in the Geocentric Datum of Australia 1994

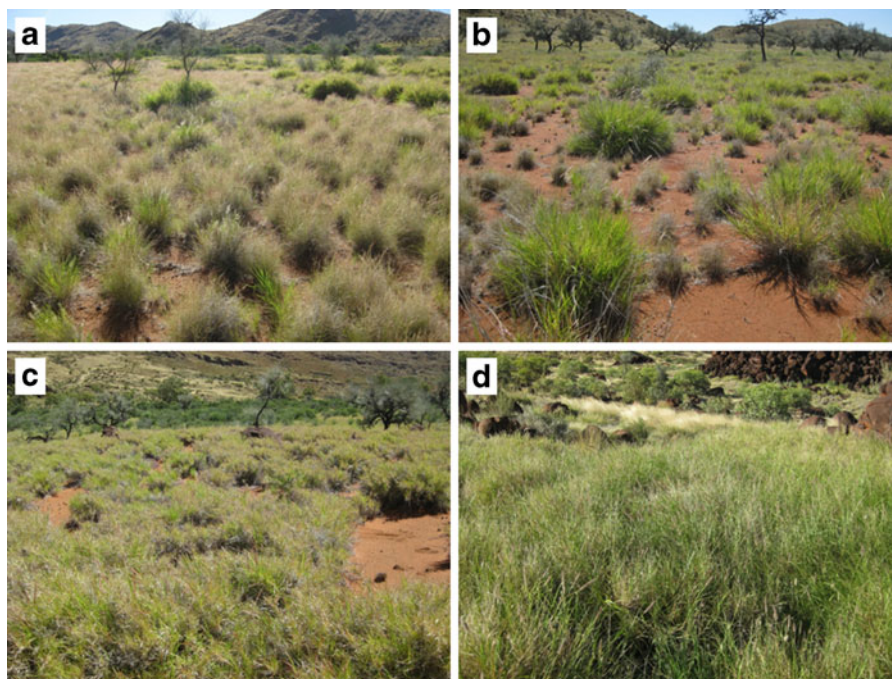


Fig. 3 Buffel grass as observed in the field at low 0–25 % (a), low–moderate 25–55 % (b), moderate–high 55–85 % (c) and high >85 % (d) projected cover. The dominant grasses in panel a are *Aristida* sp.

accurately place the site. Of the remaining sites, 43 lay within the coverage of the multispectral image scenes. Ultimately, a total of 53 and 43 sites were used for interpretation and classification of the aerial colour photography and four-band multispectral imagery, respectively.

Aerial photography image classification

We evaluated three commonly used image classification techniques for discriminating and quantifying Buffel grass in the aerial photography including visual cover estimates, manual digitisation, and a pixel-based unsupervised classification. Classifications were run separately for each field site (53 sites \times 3 approaches).

Visual cover estimates for each ground validation site were scored using the same cover classes employed in the field survey. For consistency, sites were viewed at a scale of 1:125 to make the estimates. Visual standards (Fig. 4) also aided in making observations consistent.

For the manual digitisation method, individual Buffel grass plants or clumps within the 10-m diameter circular plots were digitised from the imagery, at a display scale of 1:125 m. The digitiser did not alter the viewing scale

in order to more precisely circle plants. The total digitised area of Buffel grass for each site was then tabulated.

For the pixel-based assessment, an unsupervised classification was performed on the imagery at each site. A circular area of a diameter of 30 m, centred on the ground validation site, was used to run the classification. This accounted for the possibility to have a “Buffel grass” class even if Buffel grass was not present within the more tightly prescribed sample site. The classification was performed using the Iso Cluster Unsupervised Classification tool in ArcGIS 10 Spatial Analyst. The number of classes was set to 20; classes most representative of Buffel grass were then manually aggregated on the basis of visual examination. The aggregation process is producer-directed, allowing for some flexibility in the number of classes selected as representative of Buffel grass. The total area classified as Buffel grass for each site was then tabulated.

Four-band imagery classification

To exploit the additional spectral information in the multispectral imagery, the NDVI was applied. In the

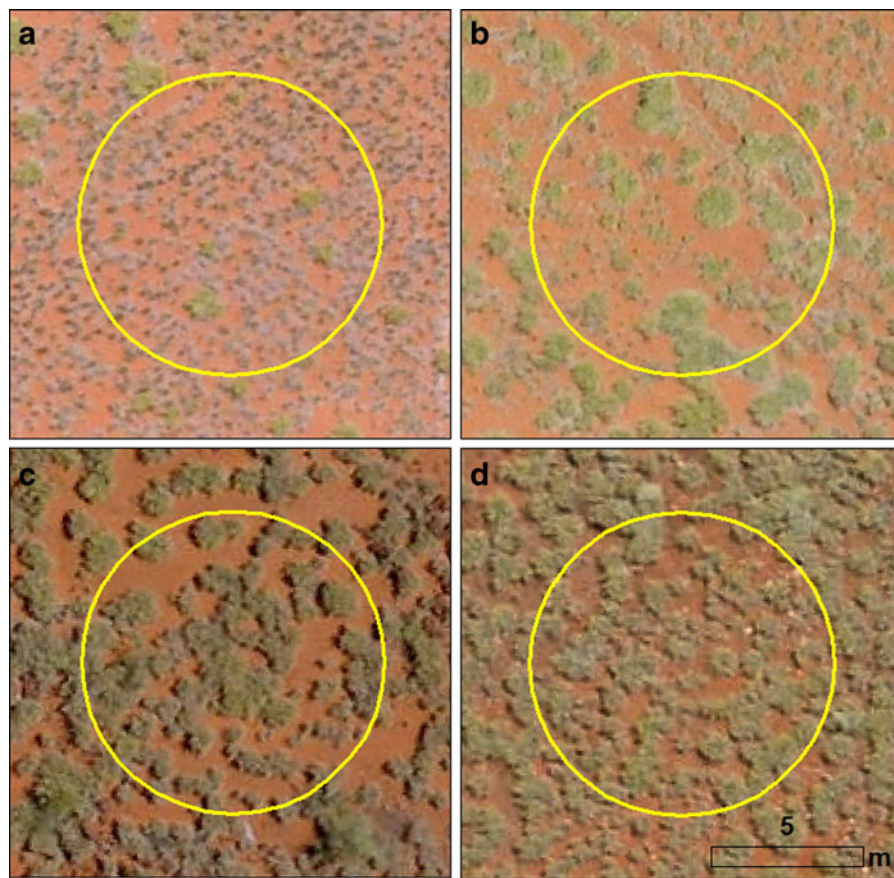


Fig. 4 Buffel grass as observed in on the 5-cm GSD colour digital photography at low 0–25 % (a), low–moderate 25–55 % (b), moderate–high 55–85 % (c) and high >85 % (d) projected cover. The dominant grasses in panel A are *Aristida* sp.

desert environment in which our study is situated, Buffel grass is often the “greenest” vegetation in the understory during the summer months (December–February). Hence, the NDVI is a suitable index to identify cover type. The NDVI output was visually compared with the higher-resolution aerial photography to identify an NDVI threshold that best represented Buffel grass cover. The total area classified as Buffel grass was then calculated for each site.

Comparing classifications

To explore differences between each of the cover estimation approaches (visual cover estimates, manual digitisation, unsupervised classification, NDVI thresholds), classification results for selected sites were viewed concurrently, and disparities were described. The effectiveness of each approach in quantifying Buffel grass cover was then examined using regression

analyses. The four image classifiers were compared not only with the field-based estimates, but with each other—to compare like with like. This is important, because whilst Buffel grass presence–absence is best interpreted from field results, field cover estimates are also subjective, and not necessarily more correct than the image-based estimates. The strength of each relationship was interpreted using Pearson's *r*-squared.

Results

Buffel grass in the landscape

Buffel grass is observed to be widespread throughout our study site. It is particularly prevalent in riparian land systems (Fig. 5, panel f) and alluvial plains (Fig. 5, panel a). In Buffel grass monocultures, on the plains comprised of undifferentiated alluvial and fluvial soils,

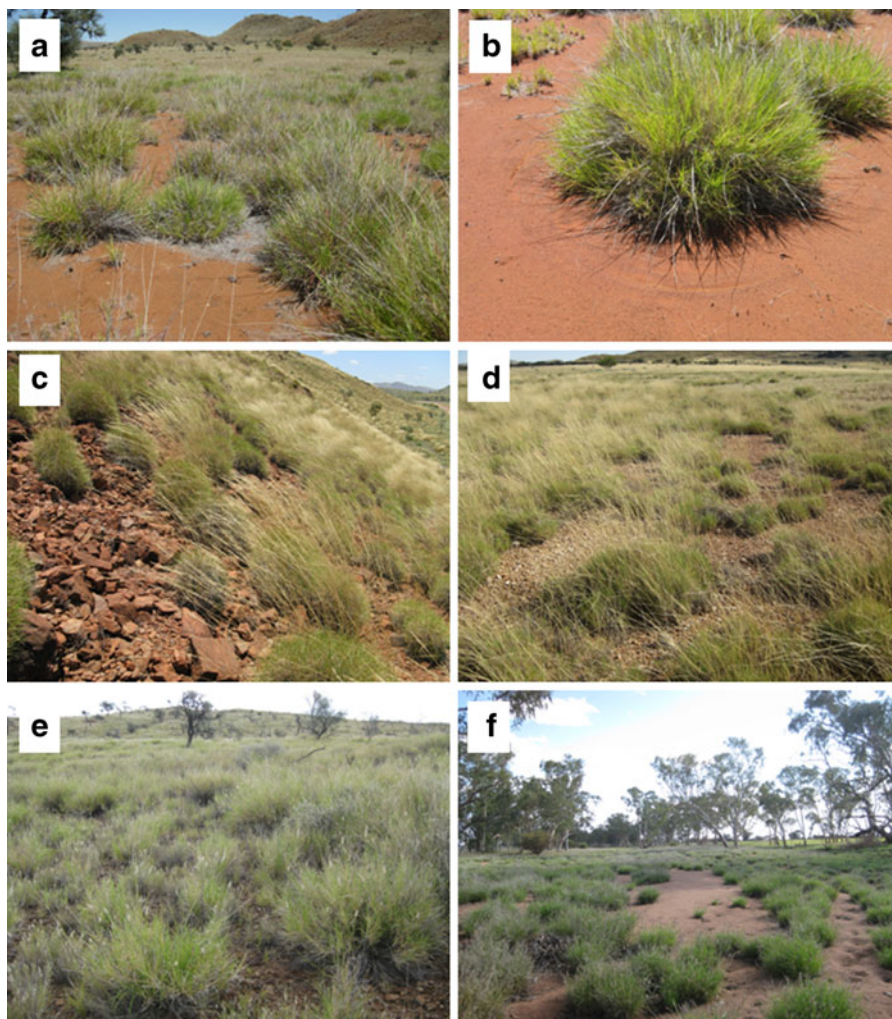


Fig. 5 Examples of the dominant landscapes within our study area. Buffel grass-dominated alluvial plain (a); mature Buffel grass tussock on alluvial plain, with bare soil surrounding it (b); Spinifex-dominated hill slope (c); Spinifex-dominated calcareous

rubble plain (d); Enneapogon intermixed with Buffel grass on ridge top (e); Buffel grass-dominated drainage line (f). Photographs captured on February 2012

Buffel grass tussocks are typically encircled by a ring of bare soil (Fig. 5, panel b), which is not seen in this land system in patches of native grasses (e.g. *Aristida*, *Enneapogon*). In the Tomkinson Ranges, Spinifex is dominant on the hill slopes (Fig. 5, panel c), but in the depressions, valleys and the crevices of rock outcrops, Buffel grass is frequently observed. This is also true for the ranges directly north of Kalka (Fig. 1). Similarly, on calcareous flats, where Spinifex dominates with minor components of Compositae, and *Ptilotus* sp. (Fig. 5, panel d), Buffel grass was observed in micro-depressions over 0.5 km away from any roadsides. On hills in the north-west of this study area, *Enneapogon*

sp. and Buffel grass often co-dominate (Fig. 5, panel e). These key land systems within the study area are represented on the panel of photographs presented in Fig. 5.

Projected cover at each site, as recorded in the field, illustrates the diversity of ground cover within which Buffel grass occurs (Fig. 6). There is a general trend that as Buffel grass increases, other grasses decrease; this is evident in Fig. 6. The figure also shows that “soil” cover type is present at all Buffel grass sites. This is consistent with field observations that in Buffel grass monocultures, the tussocks were typically surrounded by bare soil.

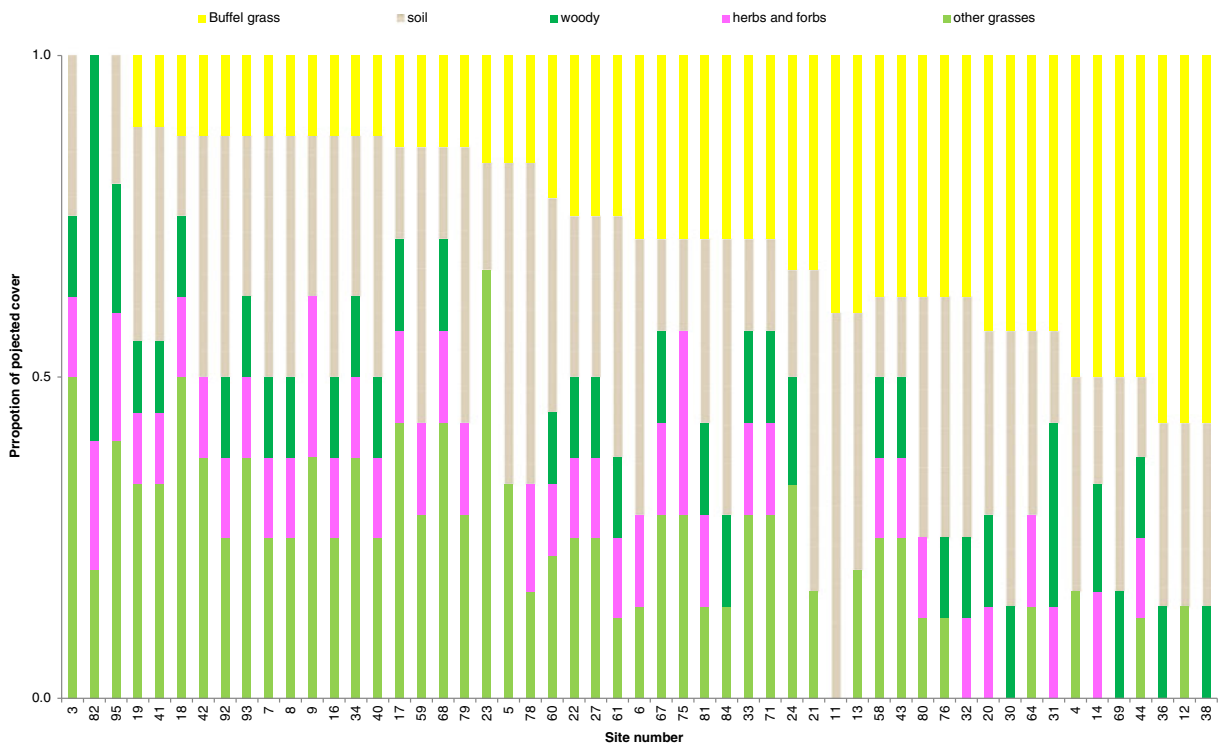


Fig. 6 Projected cover and composition of 54 field sites in the Kalka–Pipalyatjara region of far north-west South Australia. Cover types were categorically recorded as *Buffel grass*, *soil*, *woody vegetation*, *herbs and forbs* and *other grasses*. Projected

cover was categorically recorded for each cover type as “0–25 %”, “25–55 %”, “55–85 %” and “>85 %”. This graph shows the proportion of projected cover represented by each cover type for each field site

The imagery

The capacity of colour digital photography (5–6 cm GSD) and four-band Spec Terra multispectral imagery (25 cm GSD) for use in detecting Buffel grass was explored. In the aerial photography, it is possible to identify Buffel grass plants as small as 0.3 m in diameter. Larger, more mature plants ranging 0.8–2 m in diameter are easily discriminated. For large plants, the mixture of dry and green leaves, as well as shadows within the tussocks, are visible. This creates a texture, which in this landscape is quite unique to Buffel grass. In the four-band imagery, much of the internal texture of the plants is lost. Smaller plants, less than half a metre in diameter, are difficult to positively identify. Larger tussocks can be discriminated, but out of context, based on spatial information alone, they appear very similar to low shrubs. The near-infrared band was useful for discriminating Buffel grass from native Spinifex where spatial information was inadequate. The NIR band was inadequate for discriminating Buffel grass amongst native bunch grasses, such as Silky brown top (*Eulalia*

aurea), Silky blue grass (*Dichanthium sericeum*), Windmill grass (*Chloris* sp.) and Barley Mitchell grass (*Astrelba pectinata*).

Comparing projected cover estimates

Four approaches to estimate Buffel grass cover on aerial imagery were trialled: visual cover estimates, manual digitisation, an unsupervised pixel-based classification and NDVI thresholds. Figure 7 illustrates the results of the four classification methods for three ground validation sites, representative of the varying vegetation and geological settings in which we attempt to discriminate Buffel grass. Site 30 (Fig. 7, row 1) shows a monoculture of Buffel grass on red sand, typical of Buffel grass-dominated alluvial plains. Site 75 (Fig. 7, row 2) represents a transition zone from Buffel grass on alluvial plains to Spinifex hummock grass on a rocky hill slope. At this site, Buffel grass is intermixed with *Aristida* sp. and Compositae. Site 6 (Fig. 7, row 3) shows Buffel grass growing at high density along a dry creek bank, intermixed with low densities of other

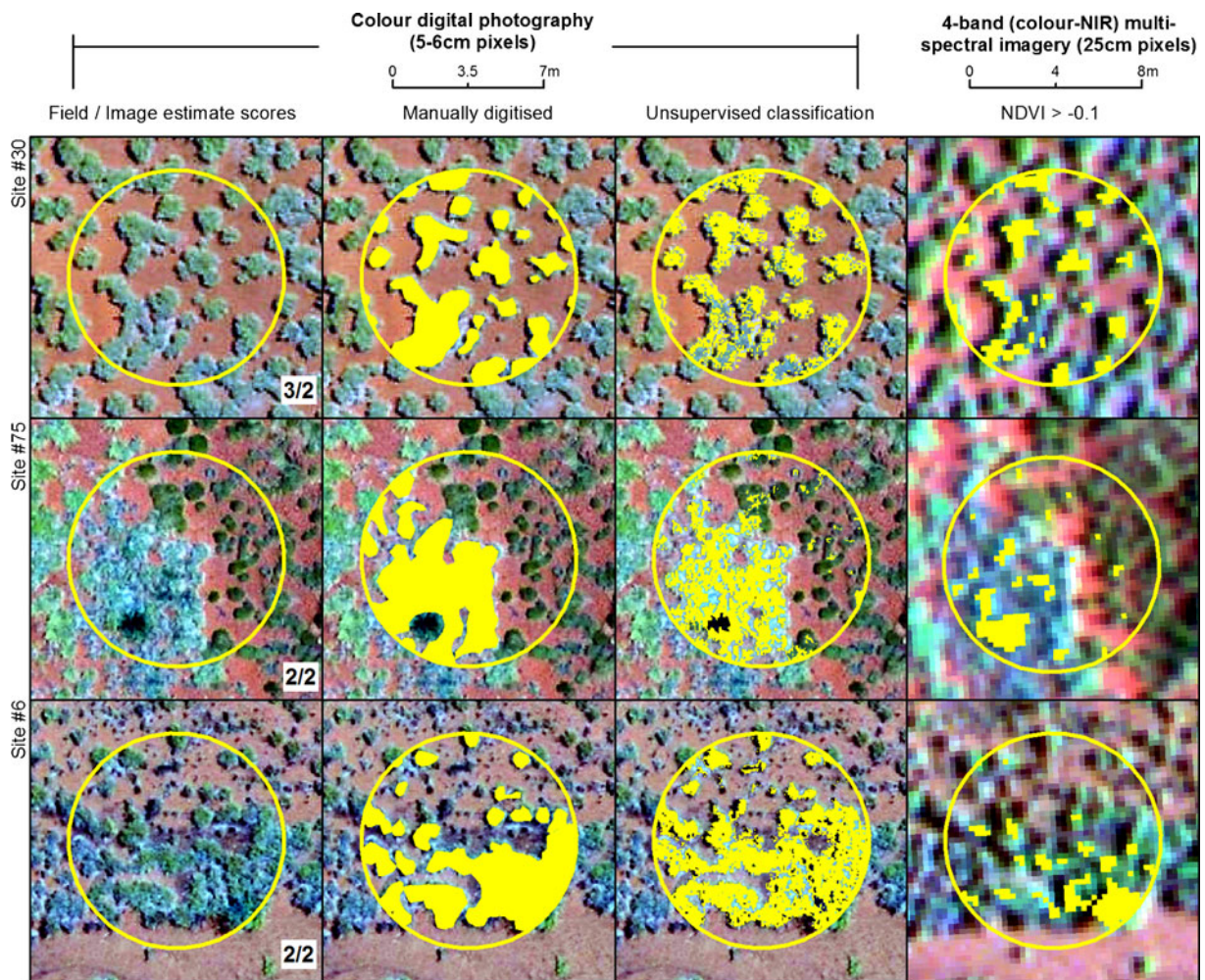


Fig. 7 Buffel grass projected cover (yellow) as estimated in the field and on the imagery by using visual cover ranking, manual digitisation of plants, unsupervised classification and NDVI thresholding, for three selected sites (field sites 30, 75, and 6). Columns 1–3 contain the colour aerial photography (~5 cm GSD) and display estimates based on this imagery. Column 4 contains

the four-band multispectral imagery (25 cm GSD), natural-colour display, and the cover estimates based on NDVI threshold. Field/image estimate scores represent the cover as “absence” (0 %) = 0, “low” (0–25 %) = 1, “moderate–low” (25–55 %) = 2, “moderate–high” (55–85 %) = 3 and “high” (>85 %) = 4

grasses such as *Themeda* sp. and *E. aurea*, which is typical of Buffel grass in creek lines.

These examples highlight some of the strengths and weakness of each classification method. Field and image estimate scores at sites 6 and 75 are equal, but at site 30, in the Buffel grass monoculture, the field estimate is one point higher than the image estimate. Considering manual digitisation, boundaries are difficult to define where canopies are touching, as evident in site 75 where a grassy mass has been categorised as Buffel grass. Boundaries are also difficult to digitise where the plants are too small; this may be the case at site 6, where there

are some newly emerging grasses not circled. The unsupervised classification has a salt-and-pepper effect caused by spectral differences between green and dry foliage within the tussocks and the similarity of Buffel grass with surrounding vegetation. It does not capture the entirety of the projected cover of the grass tussocks as discrete objects. This is evident at all three example sites, but particularly at site 75, where patches of *Spinifex* are classified as Buffel grass. However, when the sum of the classified area is averaged out across the site, the estimates are more comparable to field-based scores. Projected cover estimates based on NDVI thresholds,

using the 25-cm GSD multispectral imagery, substantially underrepresent Buffel grass.

The relationship between each classification approach was assessed using regression analyses. Every combination of classification approaches was compared, totalling 10 separate regressions, displayed in Fig. 8. The strength of each relationship was interpreted using Pearson's *r*-squared. *r*-Squared values based on the four-band imagery (NDVI thresholds) are not statistically comparable with photography-based analyses because the *n* values are different. However, the trends are comparable, and for this reason, we have presented all the regressions together. The cover, where Buffel grass was present (field cover ranking = 1–4), was comparatively lower in all image-based classification

approaches compared with field-based estimates. Where it was absent (field cover ranking = 0), the visual cover ranking and the unsupervised classification were comparatively higher than field estimates, while manual digitising and NDVI thresholds seem consistent. Image visual cover rankings are highly correlated ($r^2=0.66$) but consistently lower than corresponding manually digitised areas. Pixel-based methods (NDVI and unsupervised classification) tend to overrepresent Buffel grass absence and underrepresent presence.

Of all aerial photography image-based classifications, the visual cover ranking best correlates to results collected in the field ($r^2=0.39$). Manually digitised area consistently underrepresented Buffel grass compared with other methods; it returned a highly variable r^2

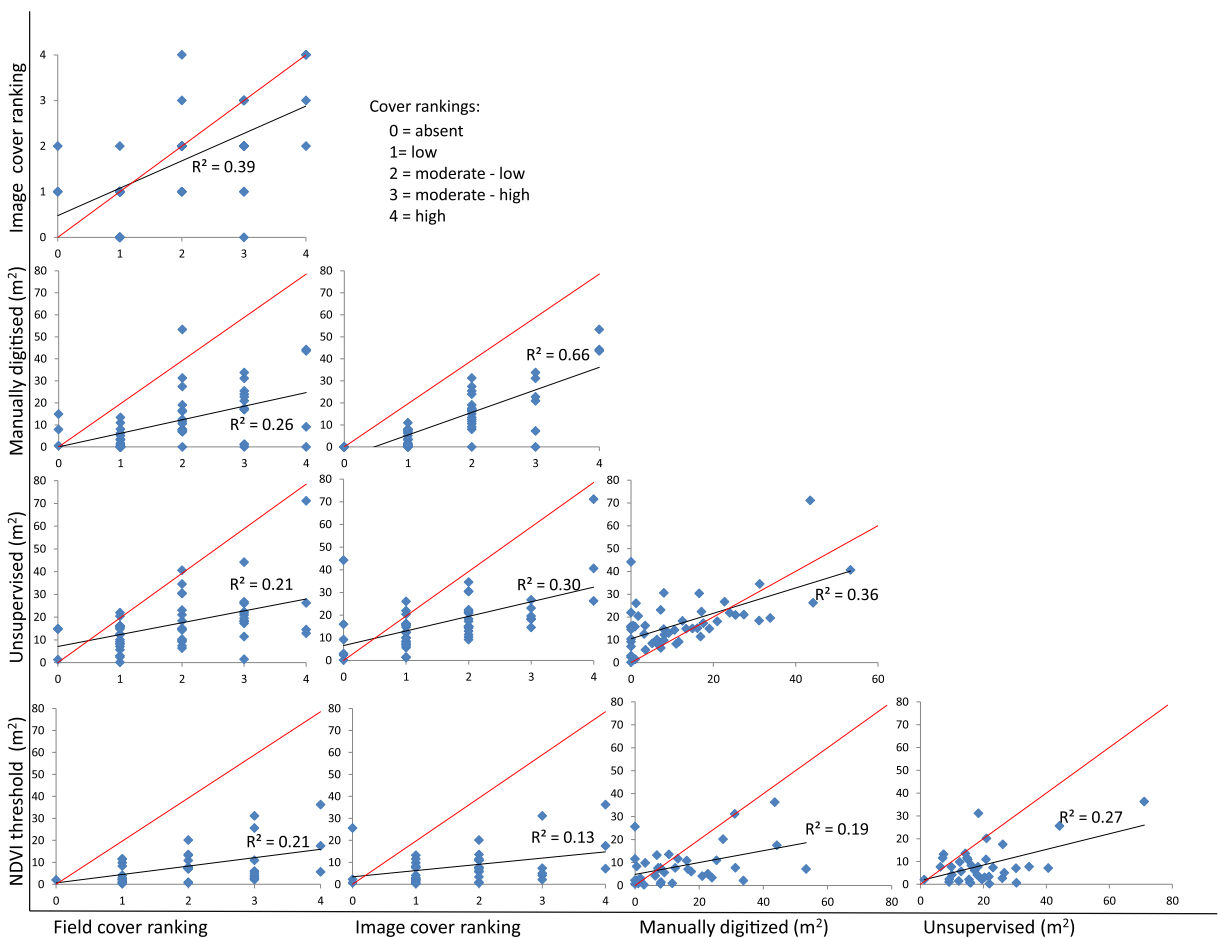


Fig. 8 Relationship between each method for estimating Buffel grass projected cover on the imagery (visual cover classes, manual digitising, unsupervised classification and NDVI threshold) and relative to field-based estimates. The strength of those relationships

is represented by Pearson's *r*-squared, presented on each graph. Projected cover ranking 0–4 represent “absent” (0 %), “low” (0–25 %), “moderate–low” (25–55 %), “moderate–high” (55–85 %) and “high” (>85 %) cover, respectively

ranging 0.26–0.66. The high-end r^2 (0.66) relates to its correlation with image visual cover rankings. The unsupervised classification correlated moderately well across the board (r^2 ranging 0.21–0.36). The NDVI thresholding approach used to classify the four-band multispectral imagery returned low ranging r^2 values of 0.13–0.27 and underrepresented Buffel grass projected cover across the board.

Discussion

Buffel grass is an invasive tussock grass widespread in arid and semi-arid ecosystems of Australia and the Americas, which homogenises landscapes, presents a tremendous fire hazard and threatens environmental and cultural values of infested regions. New infestations are where control efforts need to be focused. For control to be successful, these emerging infestations need to be detected with improved efficiency. We explored the potential of airborne imagery (ultra-high-resolution colour digital photography and four-band visible–NIR) for detection of emerging Buffel grass populations in Australian arid lands. We also compared common image classification techniques (visual estimates, manual digitisation, unsupervised digital classification and NDVI thresholding) for their suitability for discriminating Buffel grass.

Buffel grass in Kalka–Pipalyatjara

Buffel grass is observed widespread in the Kalka–Pipalyatjara region throughout our study site. Alluvial flats, once carrying a diversity of Compositae and Solanaceae members, as well as *Aristida*, and *Enneapogon* species, are now Buffel grass-dominated. This is consistent with our breakdown of projected cover at each field site, which showed a general trend of decreasing “other grasses” relative to increasing Buffel grass. In Buffel grass monocultures, on this soil type, individual tussocks are typically encircled by a ring of bare soil. We speculate that this relates to competition for water, preventing establishment of other grasses. On calcareous flats, where *Spinifex* dominates, Buffel grass was observed in micro-depressions over 0.5 km away from any roadsides, which are often a point of establishment for this invasive species (Lonsdale 1999; Van Devender and Dimmitt 2006). Similarly, on *Spinifex*-dominated hills, Buffel grass occurs in the

depressions, valleys and the crevices of rock outcrops. On hills in the north-west of this study area, *Enneapogon* sp. and Buffel grass often co-dominate, although Buffel grass has higher coverage in the creek lines through these hills. In the valley, captured by the south multispectral image, Buffel grass dominates; it is intermixed with native species at the heart of the water course, dominates with bare ground closer to the hills and gives way to *Spinifex* on the slopes.

The imagery

Colour digital photography (5–6 cm GSD) and four-band Spec Terra multispectral imagery (25 cm GSD) were compared for their capacity to discriminate Buffel grass, at the individual tussock level, in an open arid landscape.

The 5-cm GSD aerial photography was excellent for visually identifying moderate to large Buffel grass tussocks. The structural detail within the grass tussocks is only visible at the ultra-high resolution. This textural feature in the imagery made visual cover estimates easier. The GSD of 25 cm was too coarse to reveal this distinctive texture, and out of context, large tussocks could be misidentified as small shrubs. Small tussocks were indistinct to the human eye at this resolution.

Discriminating Buffel grass is most challenging when the tussocks are densely compacted, with canopies touching or when it is tightly intermixed with other species. One of the reasons for this is that the most distinctive feature of Buffel grass, for the human eye to detect, is its form. It appears as a highly textured unit, in a tight envelope of dead leaf litter, and situated in a ring of bare ground. In fact, where a Buffel grass infestation has expanded to as few as three to four mature (>1 m diameter) plants, this texture can be seen, even on viewing an image frame at its full extent. When these elements cannot be used to identify the grass, even at this very high spatial resolution, greater spectral resolution is needed.

In the NDVI thresholding classifications, we did not find the NIR band particularly helpful to distinguish Buffel grass from other bunch grasses such as Barley Mitchell grass (*Astrelba* sp.) and Silky-brown top (*E. aurea*). The NIR band may have proved more useful had the grass been at its greenest; Buffel grass was approximately 50 % dry and 50 % green at the time of image capture. Timing dependence is a weakness of classifications reliant on the NIR band. In this case, the

added spectral band does not compensate for the coarser GSD.

Classification approaches

Four approaches to estimate Buffel grass cover on aerial imagery were trialled: visual cover estimates, manual digitisation, an unsupervised pixel-based classification and NDVI thresholds. Differences between the classification outputs were visually compared, and the relationship between each classification approach was assessed using regression analyses with Pearson's r -squared.

When compared to the field estimates of cover, visual cover ranking was the best-performing image-based classifier (r^2 0.39). While perhaps the most subjective method, it is excellent for rapid assessment by a trained image interpreter. Its strength lies in the interpreter's ability to score sites rapidly and adjust interpretation according to context: image quality, vegetation condition and landscape position.

Manual digitisation of Buffel grass infestations was extremely laborious and consistently underrepresented Buffel grass-projected cover compared with all other estimation methods. Image quality is paramount to success in digitising, because slight image blur makes it extremely challenging for the digitizer to identify boundaries. Furthermore, at the individual plant level, boundaries are particularly difficult to define for small plants and for plants with canopies touching. Although it may be beneficial for the natural resource managers to have distribution information digitised, this methodology is still subjective.

The unsupervised pixel-based classification has more potential than the r^2 of 0.21 suggested. It typically underestimated cover. However, it could be just as easily overestimated cover if more “dry grass” classes were included in the producer's classification of Buffel grass. The method is reliable, systematic and repeatable; however, the process of aggregating classes' representative of Buffel grass was time-consuming when repeated for every field site. The method would be more feasible if the unsupervised classification could be applied to an entire image frame, but with aerial photography, this is challenging. Variable sun angle on the camera, resulting from aircraft tilt as it navigates topography and weather at very low altitudes (305 m, in this case), causes hot spot effects, or overexposure on sun-side edges of the imagery. This results in spectral

variation of the same land cover types across the image frame.

NDVI thresholds had potential to be a strong indicator of Buffel grass cover in this landscape. The methodology is systematic, reliable, repeatable and rapid because it can be carried out for the entire image frame. We hypothesised that a high NDVI threshold should exclude native grasses and isolate Buffel grass which is highly photosynthetically active following summer rains. However, at the time of image capture in this study, Buffel grass had already begun to dry out, and tussocks were only about 50 % green. At this time, woody vegetation had, on average, a higher NDVI than the understorey, and the NDVI values for Buffel grass were not substantially different from surrounding grasses. We chose to set a high NDVI threshold, which underrepresented Buffel grass, rather than a lower NDVI threshold, which would have captured all green vegetation. Timing dependence is a weakness of this classification method, and given the fickle nature of the species lifecycle, it is not recommended for this scale of mapping.

Conclusions

Ultra-high resolution 5-cm GSD aerial photography has potential for regional documentation of new and emerging infestations of Buffel grass. Visual cover rankings performed by an informed image interpreter are currently the most accurate method of classification. These can be conducted quickly and easily and could be expanded over a larger area with a well-designed sampling strategy to document infestations long before they are seen in the field.

For regional documentation of new and emerging infestations of Buffel grass, we recommend the following approach: (1) collect transects of aerial imagery across the region of interest. Imagery should be colour digital aerial photography with a GSD of 5 cm; (2) using the aerial photos as samples across the landscape, have a trained observer score Buffel grass cover against visual standards; and (3) use the scored sites to interpolate density across the region, target field survey and direct control efforts.

For surveillance of waterways and environments where Buffel grass is known to grow at high densities intermixed with other species, a 5-cm GSD colour digital photography together with airborne hyperspectral

imagery could be considered for improved spectral separation, and this is one area for future research.

Acknowledgments This research was undertaken as part of PhD studies at The University of Adelaide, Australia, supported by an Australian Postgraduate Award with funding and support from the Alinytjara Wilurara Natural Resources Management Board. Travel bursary awarded by the National Climate Change Adaptation Research Network (NCCARF) Terrestrial Biodiversity Network was used to carry out collaborative research at the University of Arizona. Thanks to the APY traditional owners, land managers and anthropologists for corporation and support in the swift conduct of this research project, especially April Langerak and Brad Griffiths. Thanks to Erika Lawley for invaluable assistance, cultural understanding and plant knowledge on field trips.

Open Access This article is distributed under the terms of the Creative Commons Attribution License which permits any use, distribution, and reproduction in any medium, provided the original author(s) and the source are credited.

References

- Andrew, M. E., & Ustin, S. L. (2008). The role of environmental context in mapping invasive plants with hyperspectral image data. *Remote Sensing of Environment*, *112*(12), 4301–4317.
- Blumenthal, D., Booth, D. T., Cox, S. E., & Ferrier, C. E. (2009). Large-scale aerial images capture details of invasive plant populations. *Rangeland Ecology and Management*, *60*(5), 523–528. doi:10.2111/1551-5028(2007)60[523:laicdo]2.0.co;2.
- Brenner, J. C. (2011). Pasture conversion, private ranchers, and the invasive exotic buffelgrass (*Pennisetum ciliare*) in Mexico's Sonoran Desert. *Annals of the Association of American Geographers*, *101*(1), 84–106. doi:10.1080/00045608.2010.518040.
- Brenner, J. C., Christman, Z., & Rogan, J. (2012). Segmentation of Landsat Thematic Mapper imagery improves buffelgrass (*Pennisetum ciliare*) pasture mapping in the Sonoran Desert of Mexico. *Applied Geography*, *34*, 569–575.
- Brink, A. B., & Eva, H. D. (2009). Monitoring 25 years of land cover change dynamics in Africa: a sample based remote sensing approach. *Applied Geography*, *29*(4), 501–512.
- D'Antonio, C. M. D., & Vitousek, P. M. (1992). Biological invasions by exotic grasses, the grass/fire cycle, and global change. *Annual Review of Ecology and Systematics*, *23*, 63–87.
- Franklin, K. A., Lyons, K., Nagler, P. L., Lampkin, D., Glenn, E. P., Molina-Freaner, F., et al. (2006). Buffelgrass (*Pennisetum ciliare*) land conversion and productivity in the plains of Sonora, Mexico. *Biological Conservation*, *127*(1), 62–71. doi:10.1016/j.biocon.2005.07.018.
- Ge, S. K., Carruthers, R., Gong, P., & Herrera, A. (2006). Texture analysis for mapping *Tamarix parviflora* using aerial photographs along the Cache Creek, California. *Environmental Monitoring and Assessment*, *114*(1–3), 65–83. doi:10.1007/s10661-006-1071-z.
- Gergel, S. E., Coops, N. C., & Morgan, J. L. (2010). Aerial photography: a rapidly evolving tool for ecological management. (Cover story). *Bioscience*, *60*(1), 47–59. doi:10.1525/bio.2010.60.1.9.
- Hestir, E. L., Khanna, S., Andrew, M. E., Santos, M. J., Viers, J. H., Greenberg, J. A., et al. (2008). Identification of invasive vegetation using hyperspectral remote sensing in the California Delta ecosystem. *Remote Sensing of Environment*, *112*(11), 4034–4047.
- Jia, K., Wu, B., Tian, Y., Li, Q., & Du, X. (2011). Spectral discrimination of opium poppy using field spectrometry. *IEEE Transactions on Geoscience and Remote Sensing*, *49*(9), 3414–3422.
- Laliberte, A. S., Rango, A., Havstad, K. M., Paris, J. F., Beck, R. F., McNeely, R., et al. (2004). Object-oriented image analysis for mapping shrub encroachment from 1937 to 2003 in southern New Mexico. *Remote Sensing of Environment*, *93*(1–2), 198–210.
- Lonsdale, W. M. (1999). Global patterns of plant invasions and the concept of invasibility. *Ecology*, *80*(5), 1522–1536.
- Marshall, V. M., Lewis, M. M., & Ostendorf, B. (2012). Buffel grass (*Cenchrus ciliaris*) as an invader and threat to biodiversity in arid environments: a review. *Journal of Arid Environments*, *78*, 1–12. doi:10.1016/j.jaridenv.2011.11.005.
- Mehner, H. (2004). Remote sensing of upland vegetation: the potential of high spatial resolution satellite sensors. *Global Ecology and Biogeography Letters*, *13*(4), 359.
- Meneguzzo, D. M., Liknes, G. C., & Nelson, M. D. (2012). Mapping trees outside forests using high-resolution aerial imagery: a comparison of pixel- and object-based classification approaches. *Environmental Monitoring and Assessment*, *185*(8), 6261–6275.
- Miller, G., Friedel, M., Adam, P., & Chewings, V. (2010). Ecological impacts of buffel grass (*Cenchrus ciliaris* L.) invasion in central Australia—does field evidence support a fire-invasion feedback? *Rangeland Journal*, *32*(4), 353–365. doi:10.1071/rj09076.
- Myint, S. W., Gober, P., Brazel, A., Grossman-Clarke, S., & Weng, Q. (2011). Per-pixel vs. object-based classification of urban land cover extraction using high spatial resolution imagery. *Remote Sensing of Environment*, *115*(5), 1145–1161. doi:10.1016/j.rse.2010.12.017.
- Olsson, A. D., van Leeuwen, W. J. D., & Marsh, S. E. (2011). Feasibility of invasive grass detection in a desertscrub community using hyperspectral field measurements and landsat TM imagery. *Remote Sensing*, *3*(10), 2283–2304.
- Olsson, A. D., Betancourt, J. L., Crimmins, M. A., & Marsh, S. E. (2012). Constancy of local spread rates for buffelgrass (*Pennisetum ciliare* L.) in the Arizona Upland of the Sonoran Desert. *Journal of Arid Environments*, *87*, 136–143.
- Padalia, H., Kudrat, M., & Sharma, K. P. (2013). Mapping sub-pixel occurrence of an alien invasive *Hyptis suaveolens* (L.) Poit. using spectral unmixing technique. *International Journal of Remote Sensing*, *34*(1), 325–340.
- Puckey, H., Brock, C., & Yates, C. (2007). Improving the landscape scale management of Buffel Grass *Cenchrus ciliaris* using aerial survey, predictive modelling, and a Geographic Information System. *Pacific Conservation Biology*, *13*(4), 264–273.
- Ramakrishna, N., & Steven, W. R. (1996). Implementation of a hierarchical global vegetation classification in ecosystem function models. *Journal of Vegetation Science*, *7*(3), 337–346.

- Sharif-Zadeh, F., & Murdoch, A. J. (2001). The effects of temperature and moisture on after-ripening of *Cenchrus ciliaris* seeds. *Journal of Arid Environments*, 49(4), 823–831.
- Smyth, A., Friedel, M., & O'Malley, C. (2009). The influence of buffel grass (*Cenchrus ciliaris*) on biodiversity in an arid Australian landscape. *Rangeland Journal*, 31(3), 307–320. doi:10.1071/rj08026.
- Stohlgren, T. J., & Schnase, J. L. (2006). Risk analysis for biological hazards: what we need to know about invasive species. *Risk Analysis*, 26(1), 163–173. doi:10.1111/j.1539-6924.2006.00707.x.
- Ustin, S. L., DiPietro, D., Olmstead, K., Underwood, E., & Scheer, G. J. (2002). Hyperspectral remote sensing for invasive species detection and mapping. In *Geoscience and Remote Sensing Symposium, 2002. IGARSS '02. 2002 I.E. International*, (Vol. 3, pp. 1658–1660 vol.1653).
- Van Devender, T. R., & Dimmitt, M. A. (2006). *Conservation of Arizona Upland Sonoran desert habitat. Status and threats of buffelgrass (Pennisetum ciliare) in Arizona and Sonora*. Tucson: Arizona-Sonora Desert Museum.
- Walter, V. (2004). Object-based classification of remote sensing data for change detection. *International Society for Photogrammetry and Remote Sensing Journal of Photogrammetry and Remote Sensing*, 58(3–4), 225–238.
- Wang, C., Zhou, B., & Palm, H. (2008). Detecting invasive sericea lespedeza (*Lespedeza cuneata*) in Mid-Missouri pastureland using hyperspectral imagery. *Environmental Management*, 41(6), 853–862.
- Yu, Q., Gong, P., Clinton, N., Biging, G., Kelly, M., & Schirokauer, D. (2006). Object-based detailed vegetation classification with airborne high spatial resolution remote sensing imagery. *Photogrammetric Engineering and Remote Sensing*, 72(7), 799–811.